

OCT 21 1946

~~RESTRICTED~~

3105  
PSW R-1830-94/2  
PL. 4

REFERENCE  
NACA

COPY 1

# RESEARCH MEMORANDUM

for the

Air Materiel Command, Army Air Forces

FLIGHT AND TEST-STAND INVESTIGATION OF HIGH-PERFORMANCE

FUELS IN R-1830-94 ENGINES

IV - COMPARISON OF COOLING CHARACTERISTICS OF

FLIGHT AND TEST-STAND ENGINES

By

Marcel Dandois and Milton Werner

Aircraft Engine Research Laboratory  
Cleveland, Ohio

CLASSIFIED DOCUMENT

This document contains classified information affecting the National Defense of the United States within the meaning of the Espionage Act, USC 50:31 and 32. Its transmission or communication of its contents in any manner to an unauthorized person is prohibited by law. Information so classified may be imparted only to persons in the military and naval Services of the United States, appropriate civilian officers and employees of the Federal Government who have a legitimate interest therein, and to United States citizens of known loyalty and discretion who of necessity must be informed thereof.

CONTAINS PROPRIETARY  
INFORMATION

LIBRARY COPY

OCT 4 2006

NASA GLENN LIBRARY  
CLEVELAND, OHIO

TECHNICAL  
EDITING  
WAIVED

## NATIONAL ADVISORY COMMITTEE FOR AERONAUTICS

WASHINGTON

OCTOBER 8 1946

LIBRARY COPY,

To be returned to the Library of

AIRCRAFT ENGINE RESEARCH LABORATORY  
National Advisory Committee for Aeronautics  
Cleveland, Ohio

~~RESTRICTED~~

AAA 6096  
R 9316016

NACA RM No. E6112

~~RESTRICTED~~

NATIONAL ADVISORY COMMITTEE FOR AERONAUTICS

RESEARCH MEMORANDUM

for the

Air Materiel Command, Army Air Forces

FLIGHT AND TEST-STAND INVESTIGATION OF HIGH-PERFORMANCE

FUELS IN R-1830-94 ENGINES

IV - COMPARISON OF COOLING CHARACTERISTICS OF

FLIGHT AND TEST-STAND ENGINES

By Marcel Dandois and Milton Werner

SUMMARY

The cooling characteristics of three R-1830-94 engines, two of which were mounted in a test stand and the other in a B-24D airplane, were investigated and the results were compared. The flight tests were made at a pressure altitude of 7000 feet; the test-stand runs were made at ground-level atmospheric conditions. Three cooling runs were made for each engine: variable cooling-air pressure drop, variable carburetor-air flow, and variable fuel-air ratio.

Cooling-prediction calculations applied to two test-stand and one flight R-1830-94 engines, equipped with the same instrumentation, indicated that the differences in predicted maximum and average cylinder temperature between any two engines were mainly caused by internal engine conditions. The maximum calculated temperature difference at take-off power was 49° F and occurred between the flight engine and one test-stand engine for the cylinder heads. At recommended cruise power, the maximum difference between any two engines was 16° F.

Actual cylinder temperatures of the three engines at nearly the same operating conditions of charge-air flow, fuel-air ratio, and cooling-air pressure drop paralleled predicted temperatures for the same conditions. This result was found to be true for a limited period of engine running time, this period coinciding with the time during which the cooling-correlation data were taken.

~~RESTRICTED~~

## INTRODUCTION

An investigation is being conducted at the NACA Cleveland laboratory at the request of the Air Materiel Command, Army Air Forces, with three R-1830-94 engines, one installed in a nacelle of a standard B-24D airplane and two on test stands, to correlate the knock-limited performance of these engines and to evaluate triptane as a component of aviation fuels in typical aircraft engines.

The correlation of knock-limited performance is dependent upon cylinder temperatures and cooling limitations. The cooling characteristics of the flight engine were reported in reference 1 (part I of this series of reports), which presents the results of high-performance fuel tests in R-1830-94 engines. A comparison of fuel knock limits and engine cooling limits is presented in reference 2 (part II). A comparison of 33-R and triptane-blended fuels is presented in reference 3 (part III).

The present report gives a cooling correlation for comparing cylinder temperatures, cooling-air pressure drops across the cylinders, and carburetor-air flows of R-1830-94 engines in flight and in test-stand operation, and is analogous to reference 4, which presents a comparison of flight and test-stand R-1830-90C engines.

## EQUIPMENT AND INSTRUMENTATION

Engine specifications. - The tests were conducted on R-1830-94 engines (flight, mfr. No. P-140776; test stand 1 and 2, mfr. Nos. P-138634 and P-140787, respectively). All three engines had been overhauled after varying periods of operation. Each engine was equipped with a two-speed supercharger (low gear ratio, 7.15:1; high gear ratio, 8.47:1), an 11.3-inch-diameter impeller, and a Bendix-Stromberg PD-12F7 carburetor with fuel injection at the impeller through spinner nozzles. A normal spark advance setting of 25° B.T.C. was used throughout the tests.

Engine installations. - The flight engine was mounted in the left inboard nacelle of a B-24D airplane (A.C. No. 42-40223); the other three engines in the airplane were of the standard R-1830-43 type. A conventional cowling, an exhaust manifold system with turbosupercharger, and a carburetor-air ducting with intercooler were incorporated in the installation for the flight tests.

The test-stand engines were cooled by drawing air at ground-level atmospheric conditions across the engines with an exhaust fan. A C-47A cowling was mounted on these engines. The cowl flaps

were removed to permit individual exhaust stacks to be led out radially behind the cowling. Carburetor air at ground-level conditions was furnished to the test engines through a variable-speed blower, a heat exchanger, and a 20-inch-diameter pipe.

Engine instrumentation. - The location of all thermocouples and cooling-air pressure tubes is completely described in reference 1. The instrumentation for the flight and test-stand engines was similar except for the absence of rear-spark-plug-gasket thermocouples on the test-stand engines.

Fuel flows were measured by a deflecting-vane-type fuel flow-meter in flight and by rotameters on the test stands. In flight, air-flow measurements were obtained from the observed uncompensated carburetor-metering pressure and converted to air flows by means of carburetor calibrations. On the test-stand installation, air flows were obtained by a 6-inch-diameter orifice installed in the carburetor-air duct according to A.S.M.E. specifications.

#### PROCEDURE

The method used in correlating the cooling data was that developed by Pinkel and presented in reference 5. The general procedure, the method of calculating all associated secondary data, and a sample calculation are presented and explained in reference 4.

Three series of runs (variable carburetor-air flow, variable cooling-air pressure drop, and variable fuel-air ratio) were made at an engine speed of 2250 rpm in low supercharger gear ratio at a spark advance of 25° B.T.C. Flight tests were made at a pressure altitude of 7000 feet; test-stand runs were made at ground-level atmospheric conditions.

#### Symbols

The following symbols are used in the cooling correlation:

- N engine speed, rpm
- n,m,K constants derived from cooling data
- T average engine temperature, cylinder heads or barrels, °F
- T<sub>a</sub> cooling-air stagnation temperature, °F

$T_c$	carburetor inlet-air temperature, °F
$T_g$	mean effective gas temperature, cylinder heads or barrels, °F
$T_{g0}$	mean effective gas temperature based on manifold temperature of 0° F, cylinder heads or barrels, °F
$W_c$	charge-air flow, pounds per hour/1000
$\Delta p$	average cooling-air pressure drop, inches of water
$\sigma$	ratio of cooling-air stagnation density at front of engine to NACA standard density at sea level

#### Cooling-Correlation Equations

The constants  $n$  and  $m$  were obtained by means of the method outlined in references 1 and 4, and the function  $\frac{T - T_a}{T_g - T}$  was plotted against  $\frac{W_c^{n/m}}{\sigma \Delta p}$ . A direct comparison of the lines for each engine on the same logarithmic grid is misleading because variations in exponents  $n/m$  cause differences in the value of the abscissa scales of each engine. For this reason the curves were plotted on separate logarithmic grids for each engine (fig. 1). Any comparison of engine-cooling variables that makes use of these curves must be arrived at by substituting specific values of the variables in the functions, expressed by the ordinate and abscissa scales, and by determining changes in  $W_c$ ,  $\sigma \Delta p$ , and  $T$  caused by the different curves of each engine.

The cooling variables may be analytically calculated by solving the equations defining these curves. The working equation is usually given in the form

$$\frac{T - T_a}{T_g - T} = K \frac{W_c^n}{(\sigma \Delta p)^m}$$

For ease of comparison of the variables, the constants for each engine are presented:

	K	n	m	n/m
Cylinder heads				
Flight engine	0.270	0.683	0.320	2.134
Test-stand engine 1	.274	.576	.305	1.890
Test-stand engine 2	.280	.594	.303	1.960
Cylinder barrels				
Flight engine	0.505	0.742	0.567	1.309
Test-stand engine 1	.385	.689	.469	1.470
Test-stand engine 2	.490	.566	.446	1.270

The constant  $n$  determines the degree of effect that charge-air flow has on the function  $\frac{T - T_a}{T_g - T}$  and hence on cylinder temperatures. This effect is seen to vary as much as 16 percent at the cylinder heads and 24 percent at the cylinder barrels between any two engines, which indicates differences in internal engine conditions.

The constant  $m$  determines the degree of effect of  $\sigma \Delta p$  on the function  $\frac{T - T_a}{T_g - T}$ . A variation of 5 percent at the cylinder heads between any two engines indicates a very uniform effect of cooling air upon average cylinder-head temperatures. At the cylinder barrels this difference increases to 21 percent, which indicates less uniformity of cylinder-barrel cooling between any two engines.

A comparison of the values of the constant  $K$ , or ordinate intercept of the correlation curves, is meaningless when different abscissas are used. When an average value of the exponent  $n/m$  for all three engines is used in plotting the correlation lines as in figure 2, however, a common abscissa is obtained and the intercept  $K$  becomes a measure of the relative position of the lines in the normal operating range of the engines (the cylinder-barrel curves tend to cross each other at extremely low powers). The values of  $K$  taken from figure 2 are:

Engine	Heads	Barrels
Flight	0.295	0.497
Test stand 1	.265	.419
Test stand 2	.275	.466



This method of plotting the correlation lines (fig. 2) affords direct visual comparison of the curves of each engine. The relative cylinder-temperature levels of the engines for constant power and cooling is apparent by inspection. The slopes indicate the degree of rate of change of cylinder temperature with power and with  $\Delta p$ . The curves of figure 2, however, should not be used for calculating specific values of  $W_c$ ,  $\Delta p$ , or  $T$  because of the error introduced in averaging the exponents but should serve for direct visual comparison.

#### Calculation of Mean Effective Gas Temperature

The experimental data initially used for calculating correlation equations, namely, the data at variable  $\Delta p$  and variable  $W_c$ , were taken at a constant fuel-air ratio of 0.08. A value of  $T_{g0}$  of 1086° F for cylinder heads and 536° F for cylinder barrels was assumed at this fuel-air ratio and at a reference manifold temperature of 0° F. These values were used in the computations of the correlation equations, as in references 1 and 4.

A curve of  $T_{g0}$  plotted against fuel-air ratio is useful in cooling predictions at fuel-air ratios other than 0.08. The data points for this curve (fig. 3(a)) were obtained by applying the correlation equations to widely varied test data for each engine under knocking and nonknocking conditions using 28-R, triptane-blend, and xylidine-blend fuels. These data fall within the same band of scatter irrespective of which engine was used and a curve faired through these points (fig. 3(b)) passes through the originally assumed values of  $T_{g0}$  at a fuel-air ratio of 0.08. The significance of this curve is that, if such widely unrelated data show a relatively constant variation of  $T_{g0}$  with fuel-air ratio, it may be considered usable for cooling-correlation calculations on any R-1830-94 engine.

#### Temperature Conversions

In order to use the engine cooling specifications involving maximum allowable engine temperatures in the correlation equations, which were based on average cylinder temperatures, the relation between average and maximum cylinder temperatures must be known. Average rear-spark-plug-boss temperature is plotted against maximum rear-spark-plug-boss temperature for each engine in figure 4. For

all three engines the deviations of maximum boss temperatures from the average tend to increase with increasing temperature; for the flight engine, however, this increase in deviation is less pronounced. Conversions of rear-spark-plug-gasket temperature are presented in figure 5 for only the flight engine because no gasket thermocouples were installed on the test-stand engines; this curve, however, was considered suitable for test-stand calculations involving gasket-temperature conversions.

Average cylinder-barrel temperatures plotted against maximum cylinder-barrel temperatures as measured by rear-middle-barrel thermocouples and rear-hold-down-flange thermocouples are presented in figures 6 and 7, respectively. In figure 6 the maximum middle-barrel temperatures show more nearly a constant difference from the average throughout the temperature range than cylinder-head temperatures; this difference is greatest for the flight engine. In figure 7, the deviation of maximum rear-hold-down-flange temperatures from the average increase with increasing temperature for the flight engine and test-stand engine 1 and are more nearly constant for test-stand engine 2. The conversions of rear-hold-down-flange temperature (fig. 7) show the least agreement of all maximum-to-average conversions presented in figures 4 to 7. This lack of agreement may be caused by the rear-hold-down-flange thermocouples partly reflecting cylinder-barrel temperatures and partly reflecting crank-case temperatures, which are primarily dependent on oil flow.

The relation between average rear-spark-plug-boss and average rear-spark-plug-gasket temperatures are shown in figure 8 for only the flight-engine data because of the absence of spark-plug-gasket thermocouples on the test-stand engines. This conversion (fig. 8), used in conjunction with that shown in figure 5, permits maximum rear-spark-plug-gasket temperatures to be converted to average rear-spark-plug-boss temperatures, or permits cooling-correlation calculations to be based on the manufacturer's specified maximum temperature limits (reference 6), which are given in terms of rear-spark-plug-gasket temperatures.

Average rear-middle-barrel temperature plotted against average rear-hold-down-flange temperature for the three engines is shown in figure 9 at three representative values of cooling-air  $\Delta p$ . Because individual curves for each engine at each  $\Delta p$  were fairly close together, an average of the three engines at each  $\Delta p$  is presented in figure 9 for clarity. The difference in  $\Delta p$  effect is caused by the difference in location of the rear-middle-barrel and the rear-hold-down-flange thermocouples on the cylinder.



### Comparison Calculations

Based on the cooling-correlation equations of each engine, calculations were made to isolate and to compare for each engine the three main variables affecting cooling; namely, the carburetor-air flow  $W_c$ , the cylinder-head and cylinder-barrel cooling-air pressure drop  $\sigma\Delta p$ , and the cylinder-head and cylinder-barrel temperature  $T$ . These calculations were made for four specified engine operating conditions: take-off power, 100-percent normal rated power, maximum cruise power (67-percent normal rated power), and manufacturer's recommended cruise power (44-percent normal rated power).

The engine conditions at each of the four powers are listed in table I. Part A lists the manufacturer's specified conditions (reference 6). These conditions include engine speed, manifold pressure, brake horsepower, mixture-control setting, and limiting cylinder temperatures at low supercharger gear ratio.

The four important parameters required to make the comparison calculations are listed in part B. The methods used in obtaining these parameters are:

(1) Carburetor-air flow corresponding to the manifold pressures and brake horsepowers given in part A were estimated from test-engine data and reference 7.

(2) Fuel-air ratios corresponding to the carburetor-air flows were obtained from flow-bench tests of a Bendix-Stromberg PD-12F7 carburetor, conducted by Bendix Products Division of Bendix Aviation Corporation.

(3) Available cylinder-head and cylinder-barrel cooling-air pressure drops were obtained as follows: The indicated airspeed of the airplane flying at an altitude of 7000 feet was determined for normal rated, maximum cruise, and recommended cruise powers. These values were taken from B-24D cruising control charts (reference 8). At take-off power with all four engines operating at the same conditions and a gross weight of 50,000 pounds, an indicated airspeed of 130 miles per hour was assumed. These values of airspeed were converted to airplane impact pressures, which in turn were converted to cylinder-head and cylinder-barrel pressure drops by means of flight data taken at various cowl-flap openings. A final multiplication by the density correction factor  $\sigma$  gave the  $\sigma\Delta p$  values listed in table I.

(4) Average rear-spark-plug-boss and average rear-middle-barrel temperatures corresponding to the specified maximum temperatures in part A, table I, were obtained from figures 5 to 9.

In addition to the values listed in table I, the following air temperatures were assumed: at take-off power cooling-air and carburetor-air temperatures,  $100^{\circ}$  F; at all other powers cooling-air and carburetor-air temperatures,  $60^{\circ}$  F.

The results of the following three sets of calculations at each of the four specified engine operating conditions given in table I are listed in the respective parts of table II.

A. Calculation of average and maximum rear-spark-plug-boss, maximum rear-spark-plug-gasket, average and maximum rear-middle-barrel, and maximum rear-flange temperatures obtained when maintaining carburetor-air flows and cylinder-head and cylinder-barrel cooling-air  $\Delta p$  specified.

B. Calculation of cylinder-head and cylinder-barrel  $\Delta p$ , which were necessary to maintain maximum specified cylinder-head and cylinder-barrel temperature limits with the specified carburetor-air flows.

C. Calculation of carburetor-air flows and corresponding brake horsepower, which were obtained when maintaining a cylinder-head and cylinder-barrel cooling-air  $\Delta p$  and maximum specified cylinder-head and cylinder-barrel temperatures.

Basing calculations A and B on a constant carburetor-air flow for all engines introduces an error, inasmuch as brake-specific-air-flow data indicate that the flight engine air flow was about 5 percent higher than that of the test-stand engines for a given power level. This discrepancy may be due either to internal engine differences or errors in carburetor air-flow calibrations.

#### RESULTS OF COMPARISON CALCULATIONS

A comparison of the results of each calculation shows that, at take-off power only, all three engines exceed the manufacturer's specified cylinder-head and barrel temperature limits given in reference 6. The high take-off temperatures obtained from cooling predictions based on correlation calculations, however, are those that would be attained if the assumed engine power and cooling conditions

were to be continued until temperatures stabilized. This state was never reached in actual B-24D tests because the airplane speed, assumed constant in the calculations, increased with time and the engine power was decreased to standard climb conditions a few minutes after take-off. Furthermore, a severe air temperature ( $100^{\circ}$  F) was chosen for the cooling calculations.

The greatest differences in temperature, cooling-air pressure drops, and charge-air flows occur at take-off power. At this power the average rear-spark-plug-boss temperature of the flight engine is  $33^{\circ}$  F higher than that of test-stand engine 2, which is  $16^{\circ}$  F higher than that of test-stand engine 1; the maximum difference in average rear-spark-plug-boss temperature is therefore  $49^{\circ}$  F, or a decrease of 9.3 percent from the highest temperature. At lower powers the sequence remains the same but the temperature differences decrease. For example, at recommended cruise power the average rear-spark-plug-boss temperature of the flight engine is  $7^{\circ}$  F higher than that of test-stand engine 2, which is  $9^{\circ}$  F higher than that of test-stand engine 1; the maximum difference is therefore  $16^{\circ}$  F, or a decrease of 4.7 percent from the highest temperature.

It is evident from the relative position of the lines in figure 2 that the flight engine runs slightly hotter than test-stand engine 2, which runs hotter than test-stand engine 1. The cooling-air pressure drops necessary to maintain engine operation at the temperature limits stated in table I differ by as much as 47 percent between any two engines at take-off power and by 31 percent at recommended cruise power. The carburetor-air flows and the corresponding brake horsepower attainable, if limiting temperatures and cooling-air pressure drops of table I are maintained, differ between any two engines by a maximum of 25 percent at take-off power and a maximum of 21 percent at recommended cruise power.

The preceding observations indicate that the cooling characteristics of R-1330-94 engines, when mounted in the particular test-stand installation used in these investigations, are an uncertain indication of the cooling characteristics of similar engines obtained in flight. The engine temperatures in flight can be predicted from the present test-stand engine data within  $10^{\circ}$  to  $50^{\circ}$  F, depending on the power condition. This lack of agreement in cooling of the engines is probably caused by discrepancies in carburetor air-flow measurements and internal engine conditions and might be greatly improved if the

engines were in the same condition with respect to ring wear, spark-plug conditions, and carbon deposits, and if infallible air-flow measurements were available in flight.

Installation differences between flight and test-stand engines such as cooling-air control, cowling design, and exhaust piping probably contribute to a smaller extent to the disagreement between flight and test-stand cylinder temperatures.

The actual cylinder-temperature differences of the three engines, taken at as nearly the same conditions of carburetor-air flow, fuel-air ratio, and cooling-air pressure drop as could be found among the various data, were the same as the predicted temperature differences for data taken at about the same time as the cooling-correlation data. At other times during the test period of the engines, the measured cylinder-temperature differences bore much less relation to the predicted temperature differences. Each engine was subjected to at least one overhaul during its testing period, which further indicates that normal changes in internal engine conditions during the testing period affect internal cooling characteristics and the relation of internal temperatures to external cooling.

#### SUMMARY OF RESULTS

Cooling predictions and a comparison of cooling characteristics of two test-stand and one flight R-1830-94 engines, equipped with the same instrumentation, showed the following results:

1. Under similar power and cooling conditions the average rear-spark-plug-boss temperatures attained on the three test engines differed by a maximum of 49° F at take-off power and by a maximum of 16° F at recommended cruise power (44-percent normal rated power). The cylinder temperatures of the flight engine were usually higher than those of one test-stand engine, which were higher than those of the other test-stand engine under similar power and cooling conditions.
2. From an analysis of the cooling-correlation constants, the differences in temperature level were most likely caused by internal engine differences, although different methods of measuring carburetor-air flow may also have contributed.
3. Differences in cooling-air control, cowlings, and exhaust piping between flight and test-stand engines had little effect on cylinder-temperature disagreements between these two installations.

4. A comparison of cooling prediction calculations such as was made among these three engines was accurate for a limited period of the engine running time, and actual cylinder temperatures of these engines paralleled calculated temperatures for similar power conditions during this period of time.

Aircraft Engine Research Laboratory,  
National Advisory Committee for Aeronautics,  
Cleveland, Ohio.

*Marcel Dandois*

Marcel Dandois,  
Mechanical Engineer.

Milton Werner,  
Mechanical Engineer.

Approved:

Joseph R. Vensel,  
Engineer Test Pilot.

Abe Silverstein,  
Aeronautical Engineer.

vab

#### REFERENCES

1. Werner, Milton, Blackman, Calvin C., and White, H. Jack: Flight and Test-Stand Investigation of High-Performance Fuels in Pratt & Whitney R-1830-94 Engines. I - Determination of the Cooling Characteristics of the Flight Engine. NACA MR No. E5G09, Army Air Forces, 1945.
2. White, H. Jack, Pragliola, Philip C., and Blackman, Calvin C.: Flight and Test-Stand Investigation of High-Performance Fuels in Pratt & Whitney R-1830-94 Engines. II - Flight Knock Data and Comparison of Fuel Knock Limits with Engine Cooling Limits in Flight. NACA MR No. E5H04, Army Air Forces, 1945.

3. Blackman, Calvin C., and White, H. Jack: Flight and Test-Stand Investigation of High-Performance Fuels in Pratt & Whitney R-1830-94 Engines. III - Knock-Limited Performance of 33-R as Compared with a Triptane Blend and 28-R in Flight. NACA MR No. E5H08, Army Air Forces, 1945.
4. White, H. Jack, Blackman, Calvin C., and Dandois, Marcel: Flight and Test-Stand Investigation of High-Performance Fuels in Pratt & Whitney R-1830-90C Engines. III - Comparison of Cooling Characteristics of Flight and Test-Stand Engines. NACA MR No. E5B23, Army Air Forces, 1945.
5. Pinkel, Benjamin: Heat-Transfer Processes in Air-Cooled Engine Cylinders. NACA Rep. No. 612, 1938.
6. Anon.: Operating Instructions, R-1830-94 Engine. PWA. OI. 48A, Pratt & Whitney Aircraft, Dec. 28, 1944.
7. Atkinson, A. S., Dahle, D. E., and Bullock, M. Y.: Calibration of Pratt & Whitney Aircraft R-1830-94 Engine. AEL-793, Naval Air Material Center, Naval Air Exp. Sta. (Philadelphia), Nov. 23, 1944.
8. Anon.: Flight Manual, B-24D and J Heavy Bombardment Airplane. Consolidated-Vultee Aircraft Corp., Jan. 1944.



TABLE I - OPERATING CONDITIONS FOR COOLING COMPARISONS OF R-1830-94 ENGINES  
IN FLIGHT AND TEST-STAND OPERATION

Power condition →		Take-off	100-percent normal rated	Maximum cruise (67-percent normal rated)	Recommended cruise (44-percent normal rated)
Variable	↓				
A. Manufacturer's specified operating conditions (reference 6)					
Engine speed, rpm		2800	2600	2250	1400
Manifold pressure, in. Hg absolute		52	43	31	33
Brake horsepower		1350	1100	735	480
Mixture-control setting		Auto. rich	Auto. rich	Auto. lean	Auto. lean
Limiting maximum rear-spark-plug-gasket temperature, °F		500	450	450	450
Limiting maximum rear-hold-down-flange temperature, °F		335	335	335	335
B. Parameters for cooling comparisons based on specified conditions in part A					
a Carburetor-air flow, Wc, lb/hr		9700	7700	4800	3000
b Fuel-air ratio from carburetor calibration		.100	.093	.062	.066
c Cooling-air GAP, heads, in. water		d6.0	e14.0	f9.0	g5.0
Cooling-air GAP, barrels, in. water		d5.0	e12.0	f7.0	g4.0
Limiting average rear-spark-plug-boss temperature, °F		471	428	428	428
Limiting average rear-middle-barrel temperature, °F		280	255	265	280

<sup>a</sup>Estimated from data of flight and test-stand engines for maximum cruise power, and from calibration of R-1830-94 engines for other power conditions (reference 7).

<sup>b</sup>From flow-bench test of Bendix-Stromberg FD-12F7 carburetor made by Bendix Products Division, Bendix Aviation Corporation.

<sup>c</sup>Available in B-24D airplane.

<sup>d</sup>Cowl flaps assumed to be one-third open; indicated airspeed, 130 mph.

<sup>e</sup>Cowl flaps assumed to be one-third open; indicated airspeed at 7000-foot density altitude, 220 mph.

<sup>f</sup>Cowl flaps assumed to be closed; indicated airspeed at 7000-foot density altitude, 190 mph.

<sup>g</sup>Cowl flaps assumed to be closed; indicated airspeed at 7000-foot density altitude, 145 mph.

TABLE II - CALCULATED RESULTS OF COOLING COMPARISONS OF R-1830-94 ENGINES

## IN FLIGHT AND TEST-STAND OPERATION

[Calculations based on following assumed air conditions - Take-off: cooling-air and carburetor-air temperatures, 1000 F; that for ground level. Other conditions: cooling-air temperatures and carburetor-air temperatures, 600 F;  $\rho$ , that for density altitude of 7000 feet.]

Variable	Power condition and engine	Take-off		100-percent normal rated		Maximum cruise (67-percent normal rated)		Recommended cruise (44-percent normal rated)	
		Flight	Test	Flight	Test	Flight	Test	Flight	Test
		stand 1	stand 2	stand 1	stand 2	stand 1	stand 2	stand 1	stand 2
A. Temperature comparisons assuming $W_c$ and $\Delta p$ of table I									
Average boss temperature, $^{\circ}F$		528	479	495	368	382	370	343	336
Maximum boss temperature, $^{\circ}F$		575	524	557	394	420	402	364	364
Maximum gasket temperature, $^{\circ}F$		567	511	530	383	399	385	354	345
Average middle-barrel temperature, $^{\circ}F$		354	326	326	232	238	245	225	233
Maximum middle-barrel temperature, $^{\circ}F$		381	339	346	240	252	268	234	247
Maximum rear-flange temperature, $^{\circ}F$		423	391	372	305	302	311	284	271
B. Cooling-air $\Delta p$ comparisons assuming $W_c$ and limiting temperatures of table I									
Average head $\Delta p$ , in. water		12.6	6.7	8.4	6.0	7.3	4.1	2.7	1.6
Average barrel $\Delta p$ , in. water		15.1	11.5	12.0	8.0	8.7	5.2	3.5	2.2
C. Carburetor-air flow and power comparisons assuming $\Delta p$ and limiting temperatures of table I									
Carburetor-air flow (head-temperature limit), lb/hr		6860	9130	8180	12,100	10,720	6920	9140	5180
Brake horsepower, from carburetor-air flow		940	1280	1140	1,750	1,550	953	1259	6560
Carburetor-air flow (barrel-temperature limit), lb/hr		4190	5490	4870	8300	9,950	6000	7730	4690
Brake horsepower, from carburetor-air flow		550	740	650	1200	1,450	825	1066	5950
								690	880

Estimated from data of flight and test-stand engines for maximum cruise power, and from calibration of R-1830-94 engines for other power conditions (reference 6).

NATIONAL ADVISORY  
COMMITTEE FOR AERONAUTICS

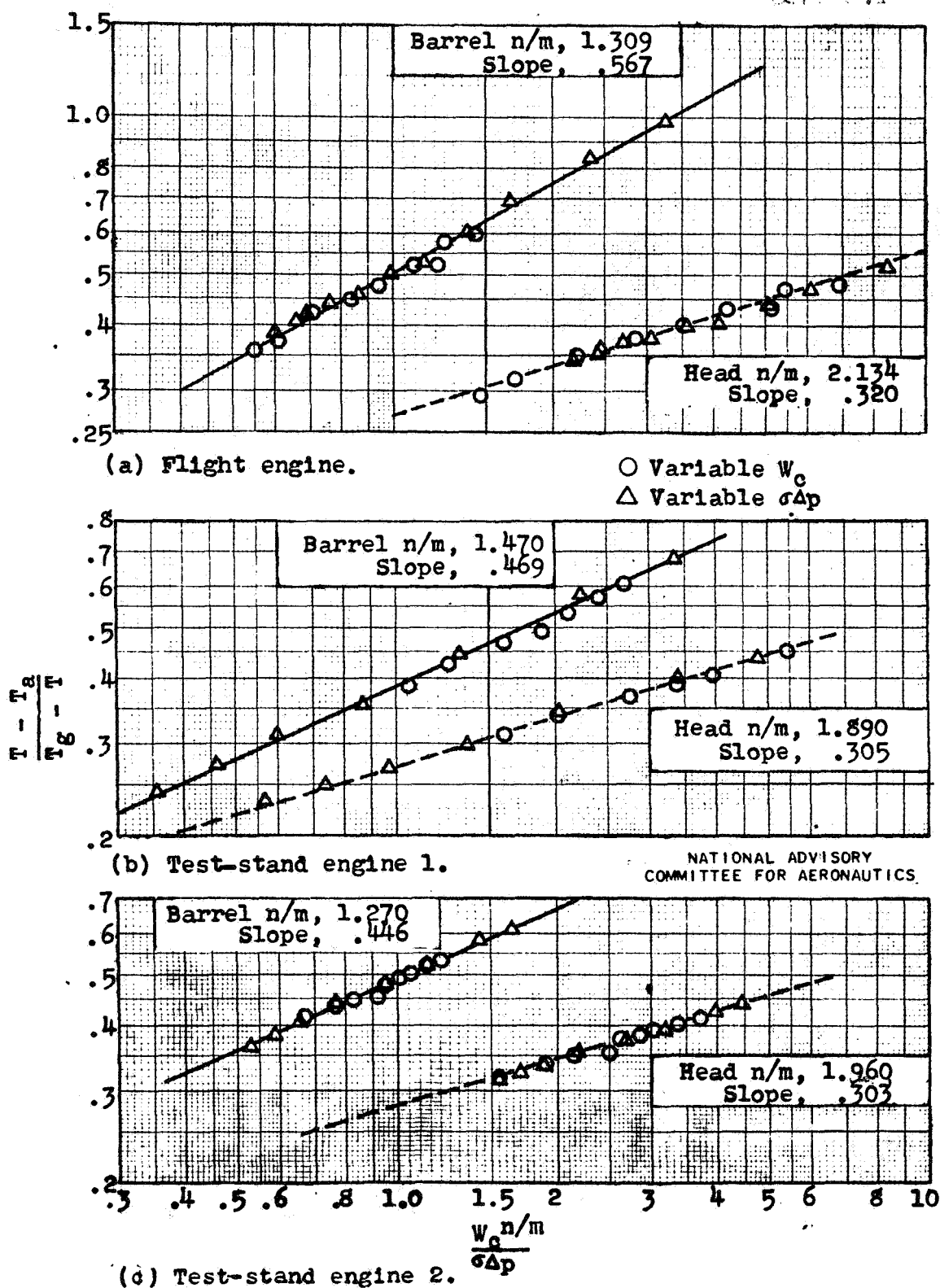
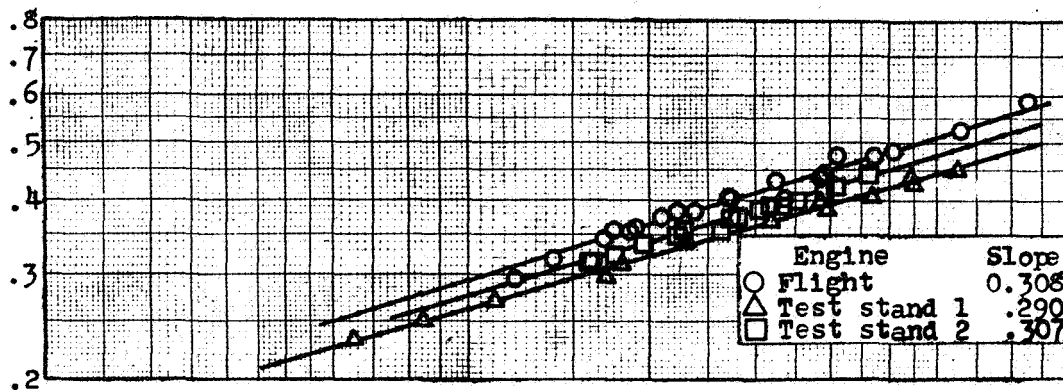


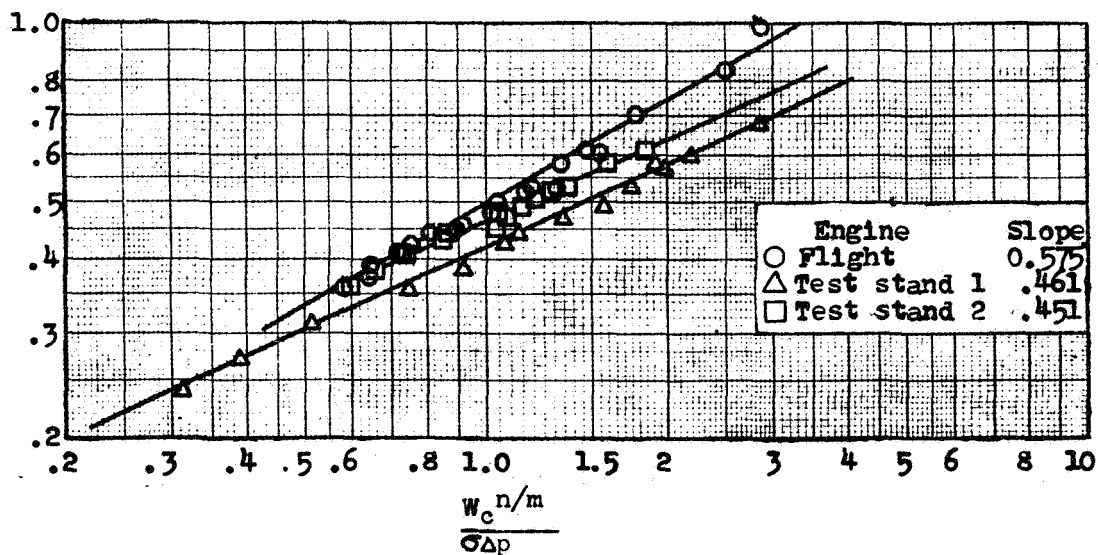
Figure 1. - Cooling-correlation curves for R-1830-94 engines in flight and in test stand. Spark advance, 25° B.T.C.



(a) Cylinder heads;  $n/m$ , 1.990.

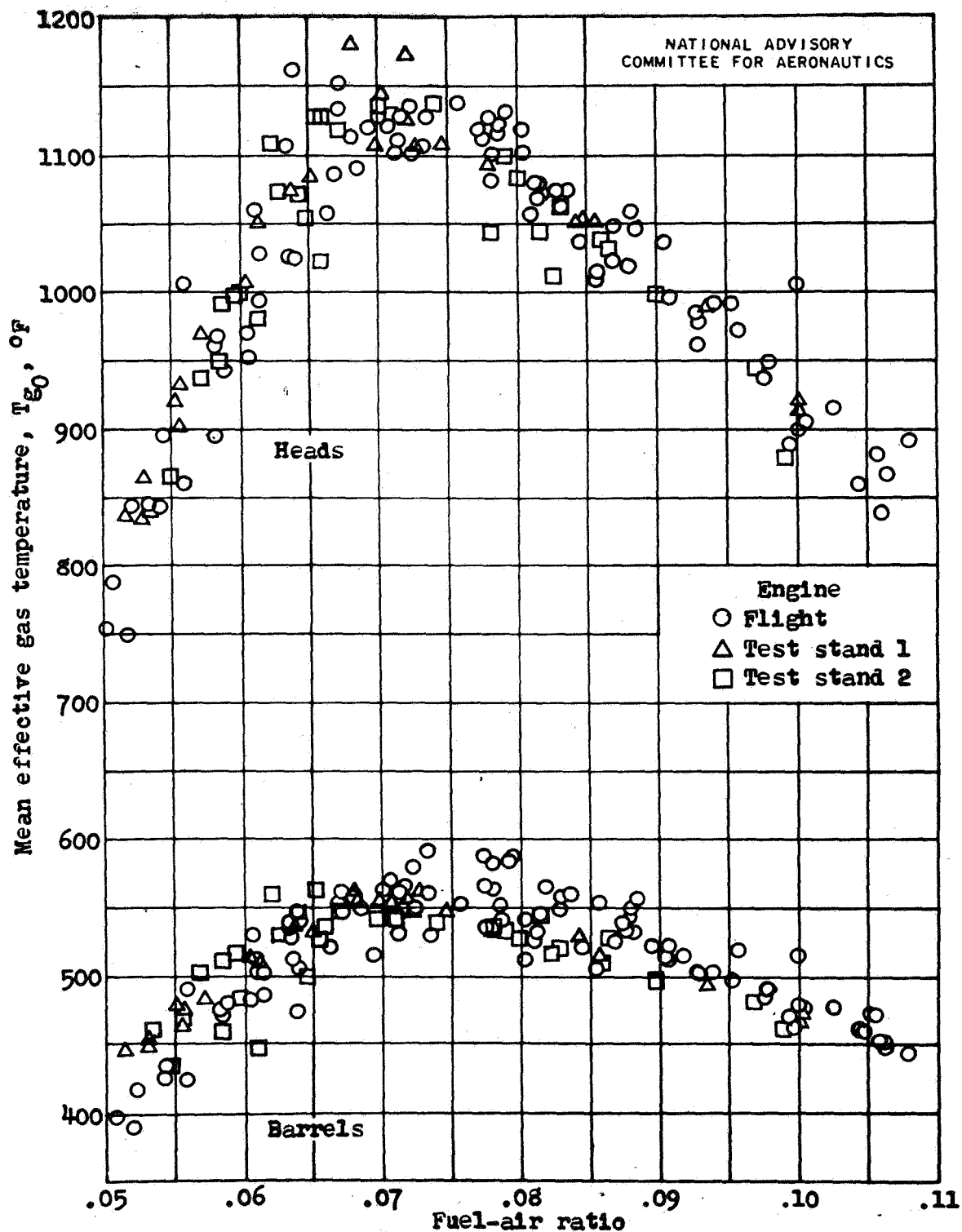
Fig. 2

NATIONAL ADVISORY  
COMMITTEE FOR AERONAUTICS



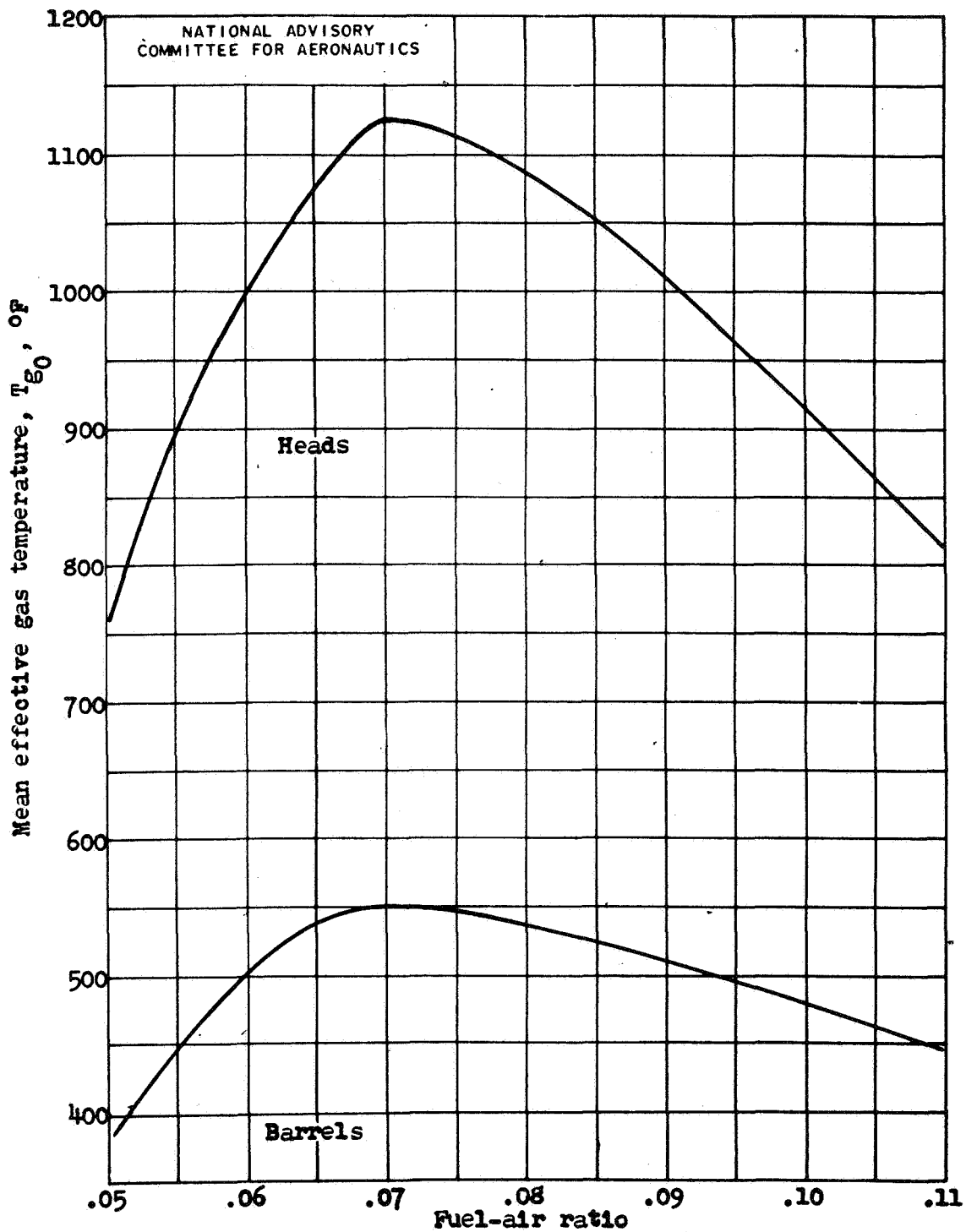
(b) Cylinder barrels;  $n/m$ , 1.350.

Figure 2. - Cooling-correlation curves for R-1830-94 engines in flight and in test stand using averaged value for exponent  $n/m$ .



(a) Test-stand and flight data.

Figure 3.- Variation of reference mean effective gas temperature  $T_{g_0}$  with fuel-air ratio. Engine speed, 2250 rpm; spark advance, 25° B.T.C.; high and low blower ratio; carburetor-air temperature, 80° to 150° F; 28-R, triptane blend, and xylydine-blend fuels.



(b) Faired curve used for prediction calculations.  
Figure 3. - Variation of reference mean effective gas temperature  $T_{g0}$  with fuel-air ratio. Engine speed, 2250 rpm; spark advance, 25° B.T.C.; high and low blower ratio; carburetor-air temperature, 80° to 150° F; 28-R, triptane-blend, and xylidine-blend fuels.



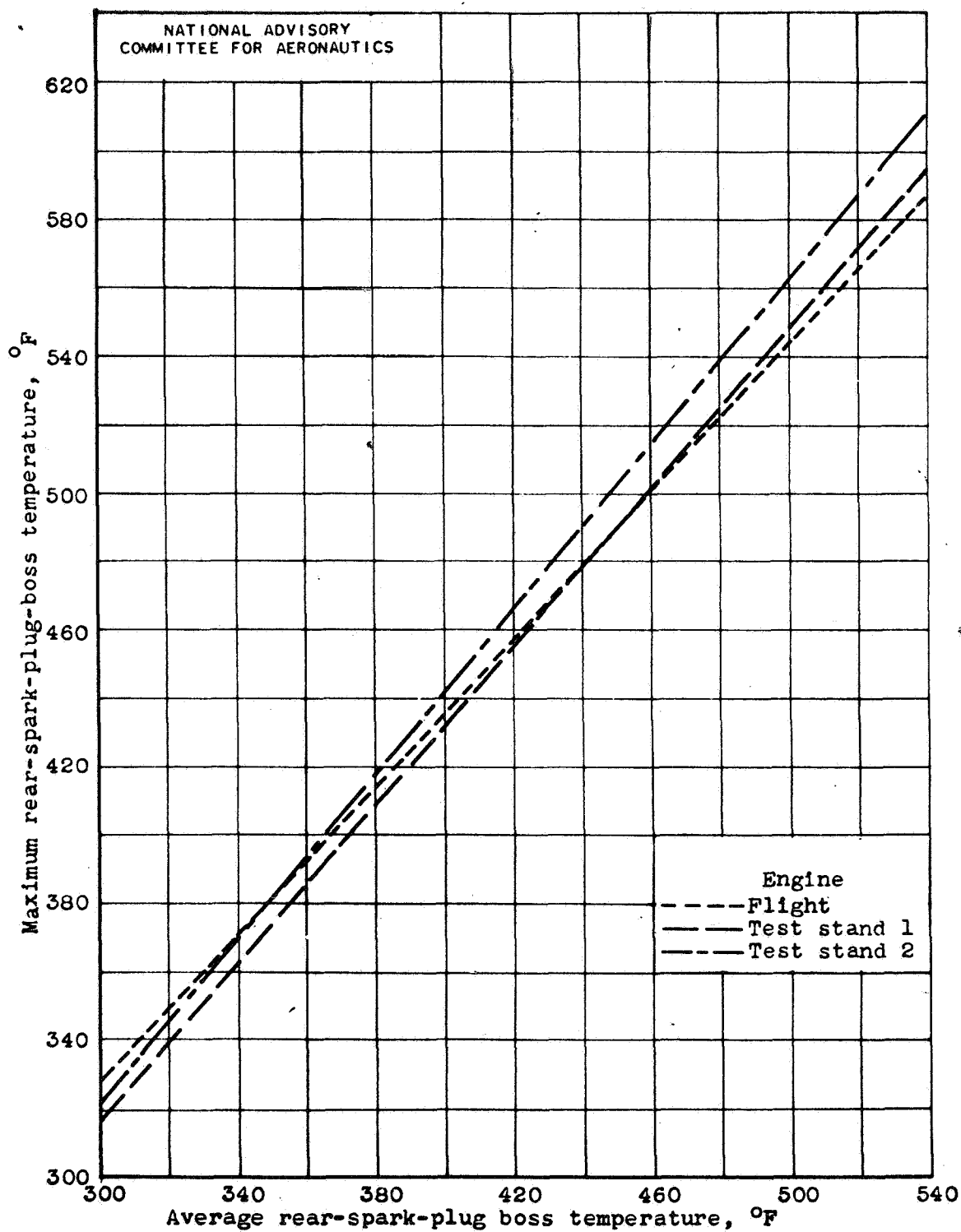


Figure 4. - Deviation of maximum from average rear-spark-plug-boss temperature measured by embedded thermocouples.

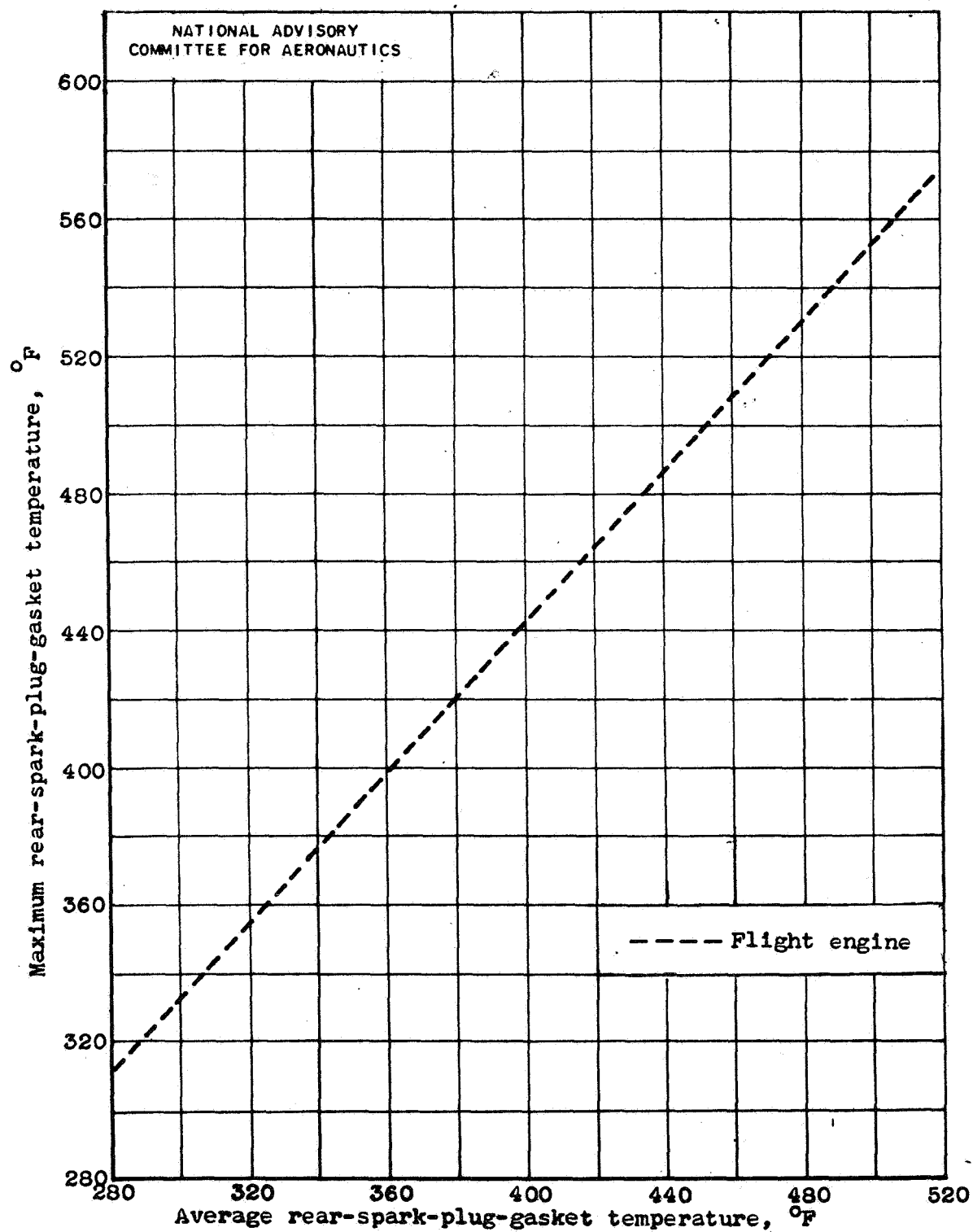


Figure 5. - Deviation of maximum from average rear-spark-plug-gasket temperature for flight engine.

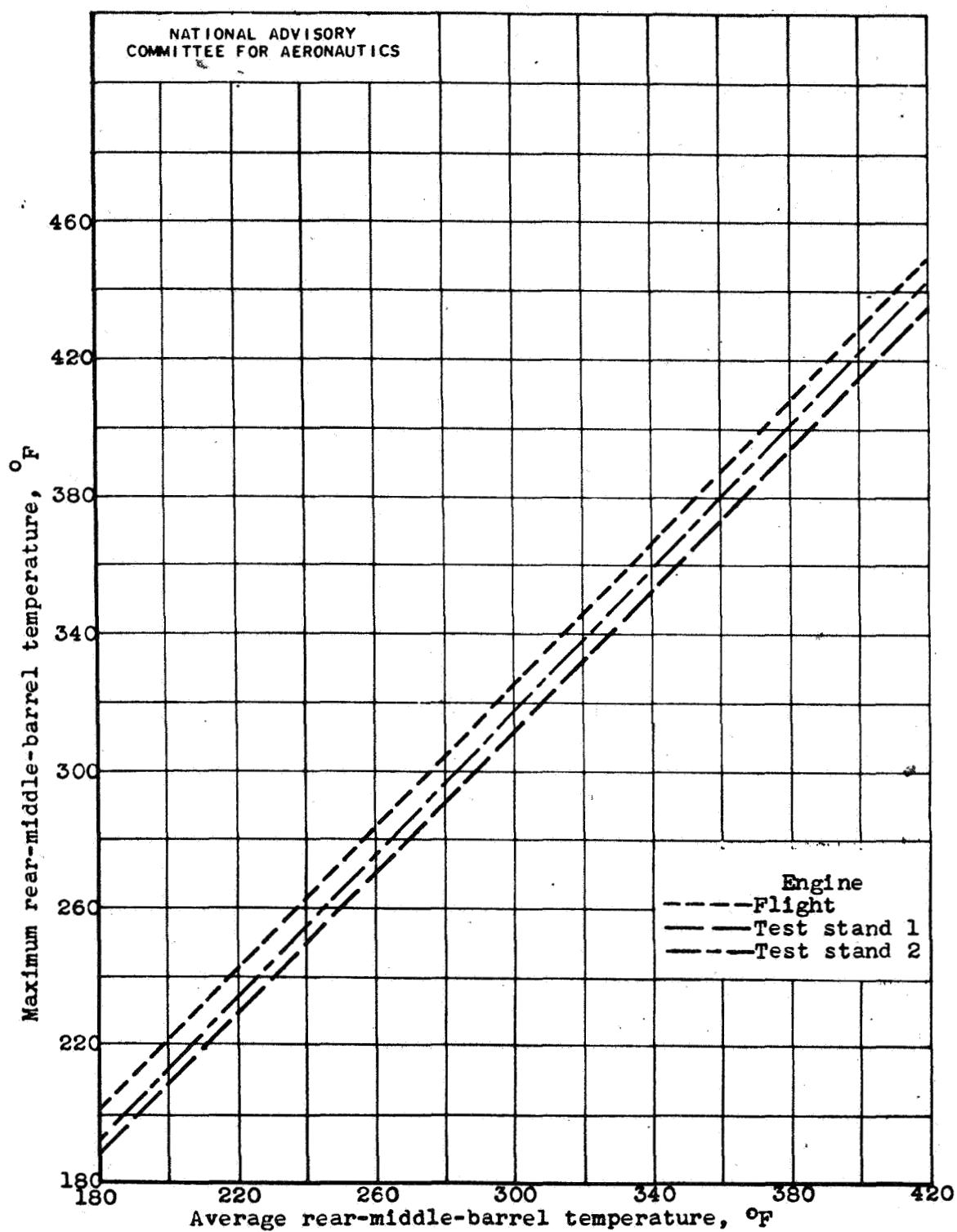


Figure 6. - Deviation of maximum from average rear-middle-barrel temperature.

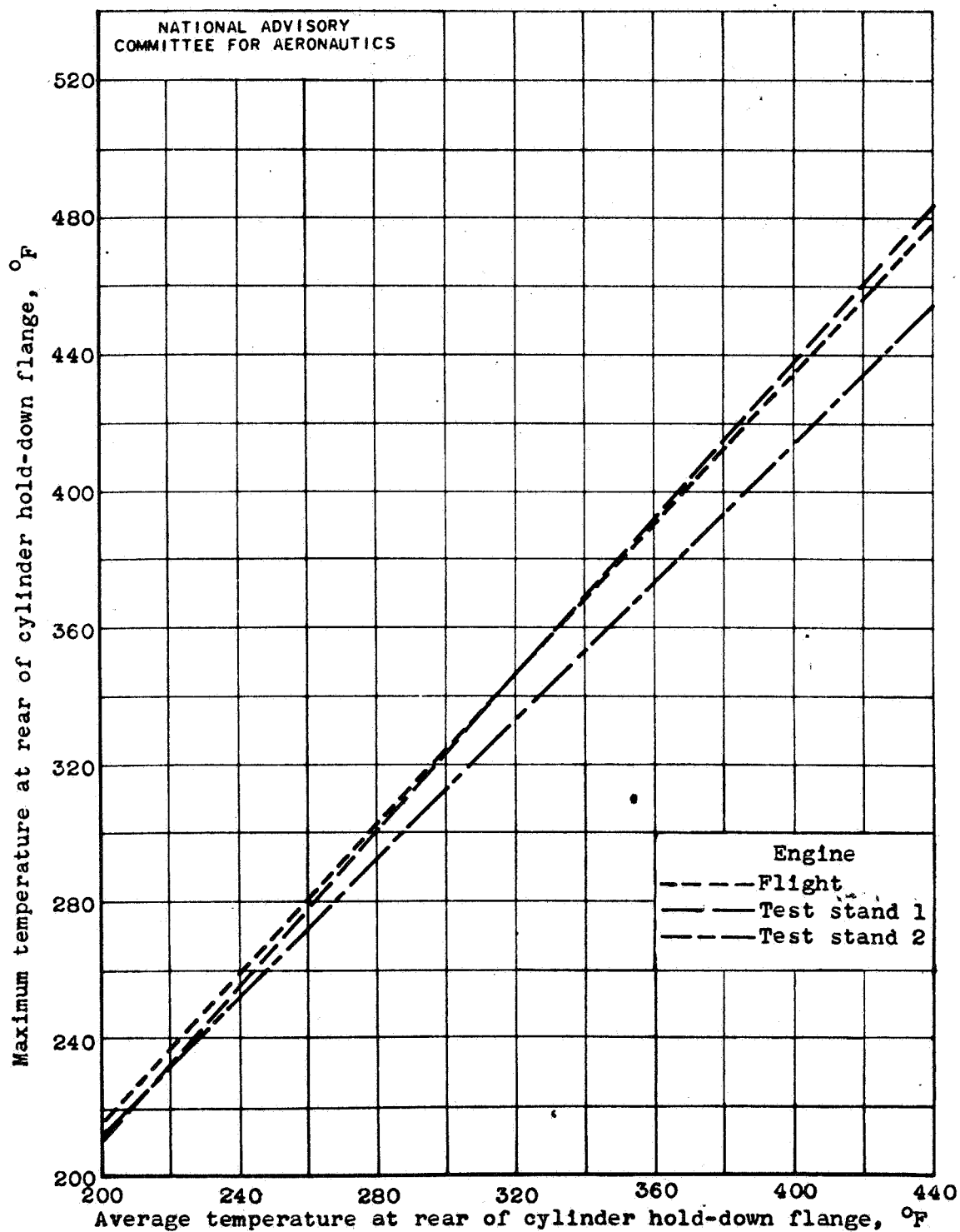


Figure 7. - Deviation of maximum from average temperature measured at rear of cylinder hold-down flange.

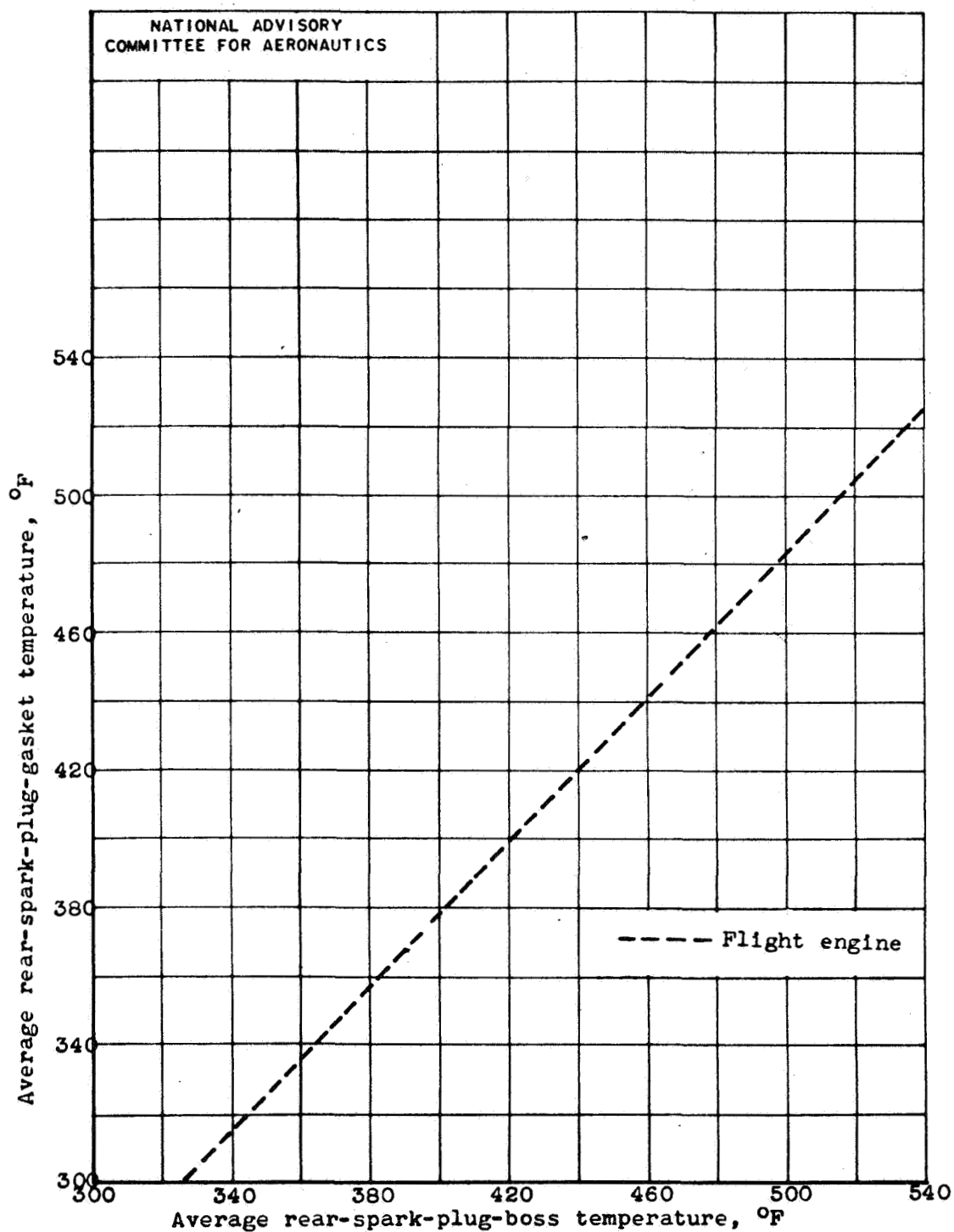


Figure 8. - Comparison of average rear-spark-plug-gasket temperature with average rear-spark-plug-boss temperature for flight engine.

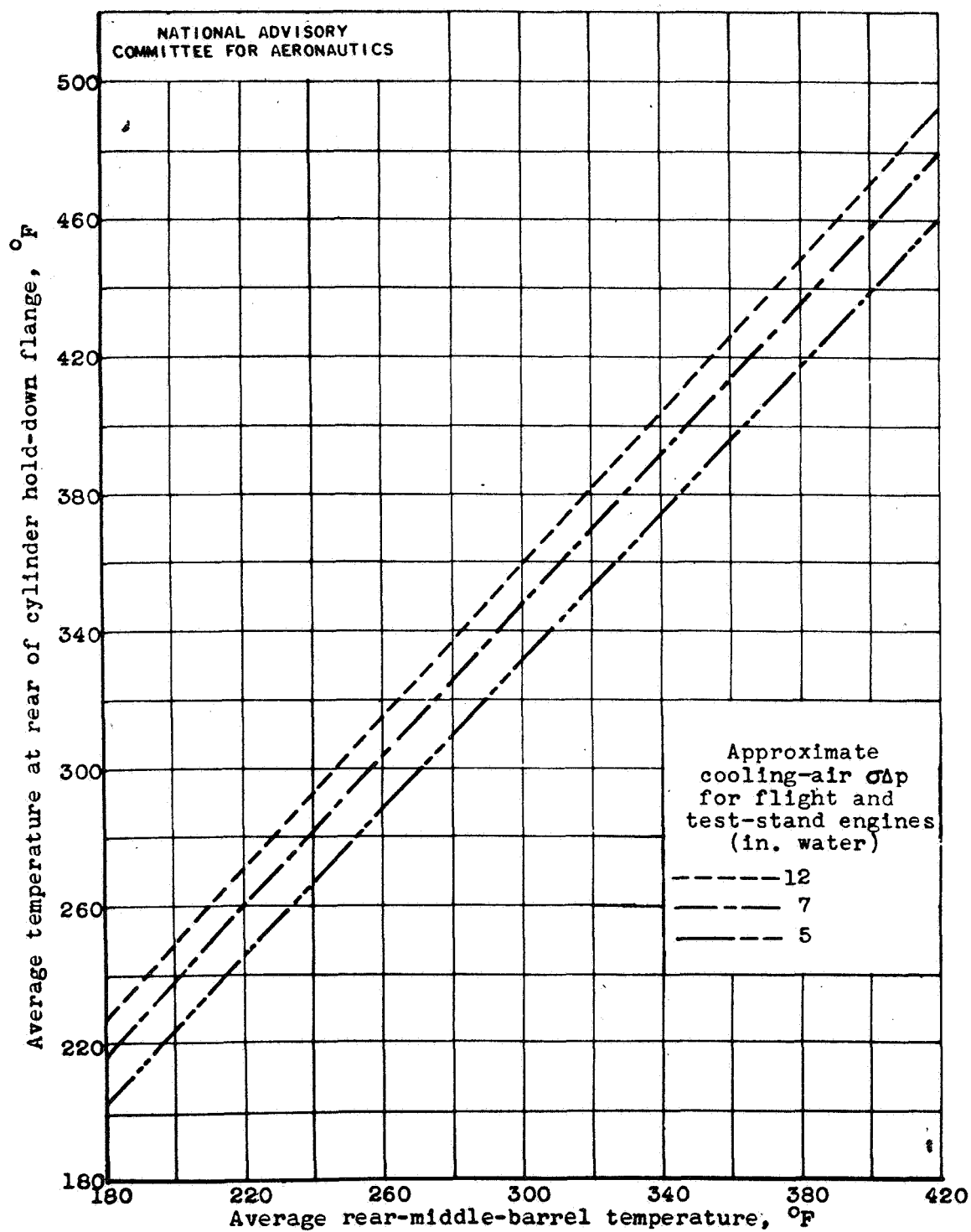


Figure 9. - Comparison of average temperature at rear of cylinder hold-down flange with average rear-middle-barrel temperature.